DIFFRACTIVE MICROSTRUCTURES WITH TWIN FOCAL POINTS

Mona MIHĂILESCU[1], Alexandru CRĂCIUN[2], Raluca Augusta GABOR[3], Cristian Andi NICOLAE[4], Mihaela PELTEACU[5], Brindus COMĂNESCU[6], George BOSTAN[7]

Here we propose a method to introduce an asymmetry coefficient to design diffractive microstructures for Fresnel lens. It determines changes of the order of sub-micrometer in the microlenses geometry. Related to the asymmetry coefficient values, we investigated the focal spots in transversal planes along propagation axis. Comparing with symmetric Fresnel lens, supplementary twin focal spots appear in a plane located at a coordinate closer to the microstructures. This behavior is proposed to be used as a new visual effect to increase the security level of holographic stamps. Some aspects from the preliminary experimental results are also presented.

Keywords: Fresnel lens, asymmetry, diffraction pattern, holographic stamps, security.

1. Introduction

Asymmetric microstructures based on the Fresnel lenses [1], axicons [2], or linear gratings [3, 4], or liquid crystals [5, 6] are used to generate beam splitters [1, 4], hollow beams [2] or for on-site surface topology measurements [3].

For optical elements placed on valuable objects or brands to protect against counterfeit attempt, structures with asymmetric linear diffraction gratings are already explored in color shifting tags [7]. Diffractive structures with asymmetric microrelief were proposed to obtain 180^0 switch effect in holographic stamps [8].

The security character is formed on holographic stamps in the design of visual effects or in the fabrication process, where quite expensive technologies are employed to reduce the counterfeit chance. For this reason, every new series of

[1] Reader, Dept.of Physics, University POLITEHNICA of Bucharest, Romania, e-mail: mona.mihailescu@physics.pub.ro
[2] Student, Faculty of Computer Science, Romania, e-mail: alex.sever@yahoo.com
[3] Eng., National Institute for Research in Chemistry, Romania, e-mail: raluca_gabor@icechim.ro
[4] Eng., National Institute for Research in Chemistry, Romania, e-mail:cristian_nicolae@icechim.ro
[5] Eng., S. C. Optoeloctronica 2001 S.A., Romania, e-mail: mihaela@optoel.ro
[6] Eng., S. C. Optoeloctronica 2001 S.A., Romania, e-mail: brindus@optoel.ro
[7] Eng., S. C. Optoeloctronica 2001 S.A., Romania, e-mail: george@optoel.ro

holographic stamps requires new elements to increase the security level. These elements are of two kinds: 1) alphanumeric characters with submicrometric dimensions in a place known only by the designer and 2) new diffractive elements which provide unique visual effects when are illuminated in white light.

To combine these two requirements, we propose a method to generate asymmetric Fresnel lenses (AFL) with consequences: i/ changes of the order of hundred nanometers to few micrometers in their geometries, imperceptive by the human eye and ii/ visual effects as supplementary twin focal spots in a plane perpendicular to the propagation axis. We investigated the changes in the geometries of Fresnel lenses induced by the asymmetry coefficient (AC) related to the changes in the focal spots. We propose these as new elements to proof of concept experiment for enhanced security features to be exploited for holographic stamps used as anti-counterfeit item on valuable objects.

In the next section, the method to design Fresnel lenses is described and the asymmetry coefficient is introduced. The intensity distribution in the diffraction pattern is analyzed in planes transversal on the propagation axis; the simulation results are described in the section 3. Some preliminary experimental results are presented in the section 4. We will end with discussions and conclusions.

2. Asymmetric diffractive Fresnel lenses design

Classical diffractive Fresnel lenses (FLs) are generated in accordance with their characteristic equation [9]:

$$r_a^2 = 2f \cdot a \cdot \lambda \tag{1}$$

which links their geometrical parameters (zone index, a, and zone radius, r_a) in a relation with the optical parameters (the focal distance f and the wavelength λ). Implementing this equation in MATLAB, a 600x800 matrix is generated with two values corresponding at two step microrelief of the obtained microlens.

Here we propose asymmetric Fresnel lenses (AFLs) designed by entering an asymmetry coefficient (AC) in the eq. 1. In this way, is obtained a displacement in the centers of half of the circles (for odd values of the zone index a) in one direction, while the others remain centered in the middle of the matrix. The values for AC were chosen such that the changes in microstructures geometry are between hundred of nanometers to few micrometers. These are limit values to obtain visual effects in the focal spot (as will be detailed further) while the displacement in the AFLs geometry to be hardly perceptible by the human eye. The AFLs presented in Fig. 1a-c, were designed for different values of AC: a) 0.9 μm, b) 5 μm, c) 8 μm as two-levels phase elements with transmittance function $t(x, y)$.

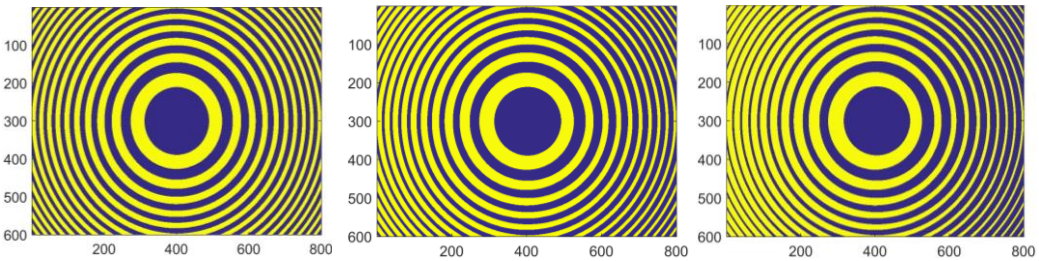

a) b) c)

Fig. 1 AFLs designed with different values of AC: a) 0.9 μm , b) 5 μm, c) 8 μm.

3. Diffraction pattern simulation

To perform the simulations for field propagation, we work in the scalar diffraction theory, Fresnel approximation. We consider a monochromatic, unit amplitude plane wave (wavelength λ), normally incident on AFL with the transmittance function $t(x, y)$ situated at $z = 0$, in the input plane. The transmittance function is generated in accordance with eq.1 where given value for AC is introduced; it is considered a binary phase diffractive element.

The complex diffracted field $U(x_z, y_z, z)$ at the distance z from the AFL, can be expressed using the 2-D convolution operator [10]:

$$U(x_z, y_z, z) = t(x, y, 0) \otimes h(x, y, x_z, y_z, z) \tag{2}$$

where

$$h(x, y, x_z, y_z, z) = \frac{\exp(ik \cdot s_{01})}{i\lambda \cdot s_{01}} \tag{3}$$

is the impulse response function, x, y are the coordinates in the input plane, the AFL plane, x_z, y_z are the coordinates in the output plane, the diffraction pattern plane (or the image plane), $k = 2\pi / \lambda$ and s_{01} is the distance between any two points from the input plane to the output plane.

In the Fresnel approximation, the impulse response function from Eq. (3) has been written for convolution operator and the complex amplitude of the diffracted field is:

$$U(x_z, y_z, z) = \frac{\exp(ikz)}{i\lambda z} \exp\left\{\frac{ik}{2z}\left[x_z^2 + y_z^2\right]\right\} \cdot \int_{-\infty}^{\infty}\int_{-\infty}^{\infty} U'(x, y, 0) \exp\left[-i2\pi(xu + yv)\right] dxdy = O_{Fre}\left(t(x, y, 0)\right) \tag{4}$$

where

$$U'(x, y, 0) = t(x, y, 0) \exp\left\{\frac{ik}{2z}\left[x^2 + y^2\right]\right\}, \tag{5}$$

and $O_{Fre}\left(t(x,y,0)\right)$ express the Fresnel transform operator, which is applied to the transmittance function of AFL and changes the variables (x, y) into the spatial frequencies: $u = x_z / \lambda z, \mathrm{v} = y_z / \lambda z$.

In simulations, we sampled these functions at Nyquist frequency, taking care on the under-sampling, and implementing Eqs. (4) and (5) in discrete form using 2-D matrices and the Fast Fourier Transform (FFT) routines in MATLAB. The simulations were performed using the built-in MATLAB functions with the discrete variables (m,n), (m_z,n_z): $x = m\cdot\Delta p$, $y = n\cdot\Delta p$, $x_z = m_z\cdot\Delta p_z$, $y_z = n_z\cdot\Delta p_z$, where Δp and Δp_z, are the pixels dimensions in the AFL plane and in the image plane respectively. The link between them is given in [11]. By denoting with M the total number of pixels in both x and x_z directions, and with N the total number of pixels in y and y_z directions (M = 1024, N = 1024), then $m = \overline{1,M}$ and $n = \overline{1,N}$. Our implementation of the Fresnel approximation in MATLAB is largely described elsewhere [12].

The transmittance function $t(x,y)$ is also used in its discrete form and corresponds to the phase mask of the diffractive AFLs.

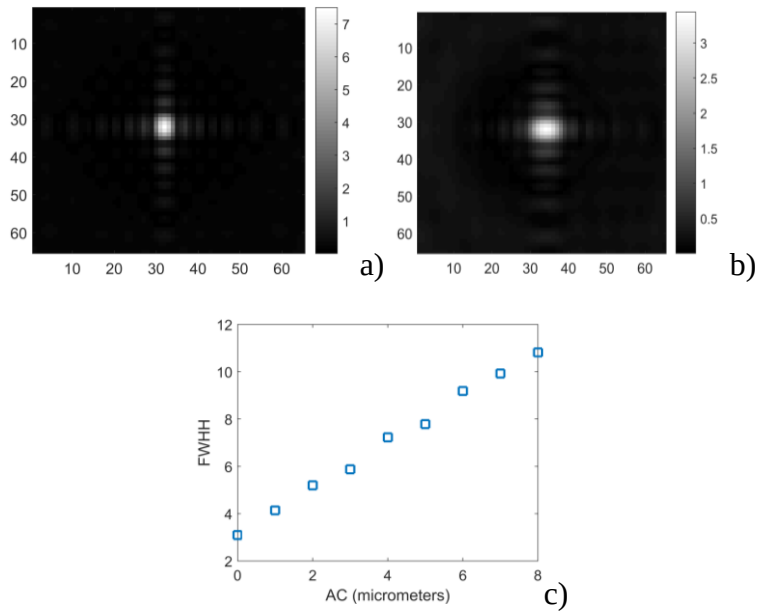

Fig. 2 Intensity distribution in planes perpendicular to the propagation axis at z_f for AC: a) 0, b) 4.25. c) Dependence between FWHH and AC

We collected sections as intensity distribution in planes perpendicular to the propagation axis. Three cases are distinct:

1. For symmetric Fresnel lens, one focal point is observed (Fig. 2a), at distance z_f along propagation axis, corresponding with given parameters in eq. 1. ($z_f = f$)

2. For AFL designed at the same parameters, a focal point is observed at the same distance z_f (Fig. 2b) but with greater values for full width at half height FWHH as AC increases (Fig. 2c);

3. Supplementary, for the same AFL, in a transversal plane situated at the distance $z_{tf} < z_f$, are observed twin focal points (Fig. 3 a-d), more distant as AC increases (Fig. 3 e).

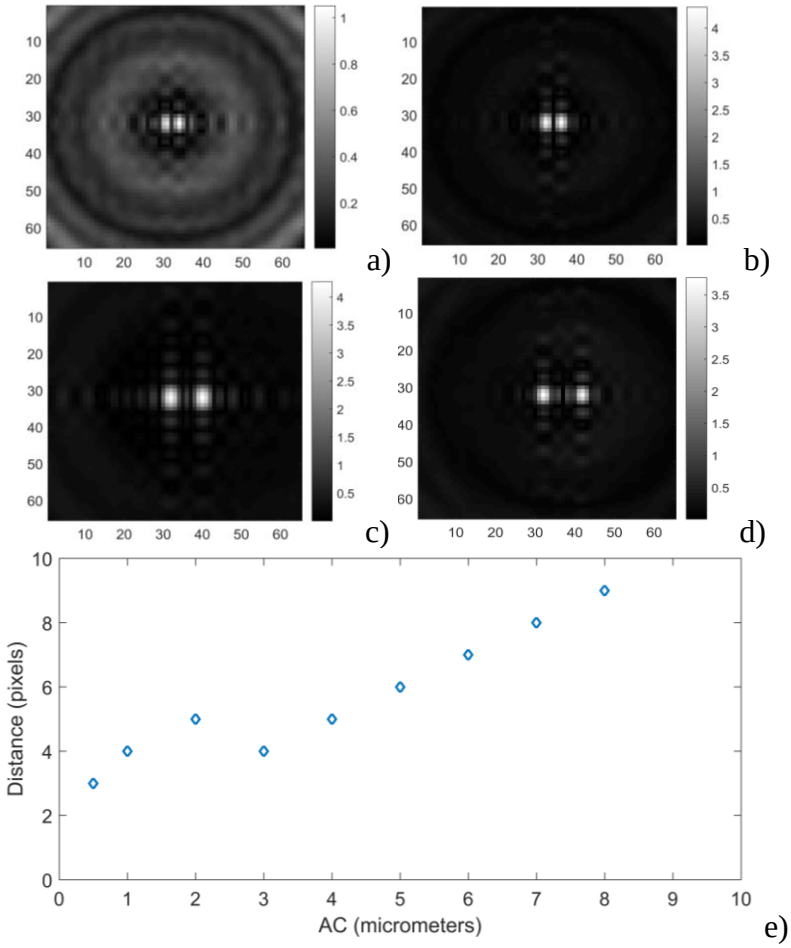

Fig. 3 Intensity distribution in planes perpendicular to the propagation axis at z_{tf} for AC: a) 0.5, b) 4.25, c) 8, d) 10. e) The distance between focal points related to AC

In all images from Fig. 2 and Fig. 3, the colorbar from the right represents the values for the intensity in arbitrary units, relative at each case.

4. Experimental analysis

These simulations results are compared with the experimental ones, by encoding the calculated phase pattern of AFL onto liquid crystal spatial light modulator, LC 2002 (HoloEye GmbH, transmission type, pixel pitch 32μm, 600x800 pixels). In our experimental setup, a laser beam (wavelength 635nm) is expanded (20mm diameter) by a telescope, and illuminates the spatial light modulator display. The diffraction patterns from different AFL are observed on a screen placed perpendicular to the propagation axis and recorded on a CCD sensor (Ophir-Spiricon. LLC, BGP-USB-L11059 Beam Profiling Camera).

In the Fig. 4 is presented an experimental image captured in a plane transversal to the propagation axis located at z_{tf}. The cursors position was chosen to highlight two maxima and the minimum between them. An additional lens was used to magnify the image of the spots.

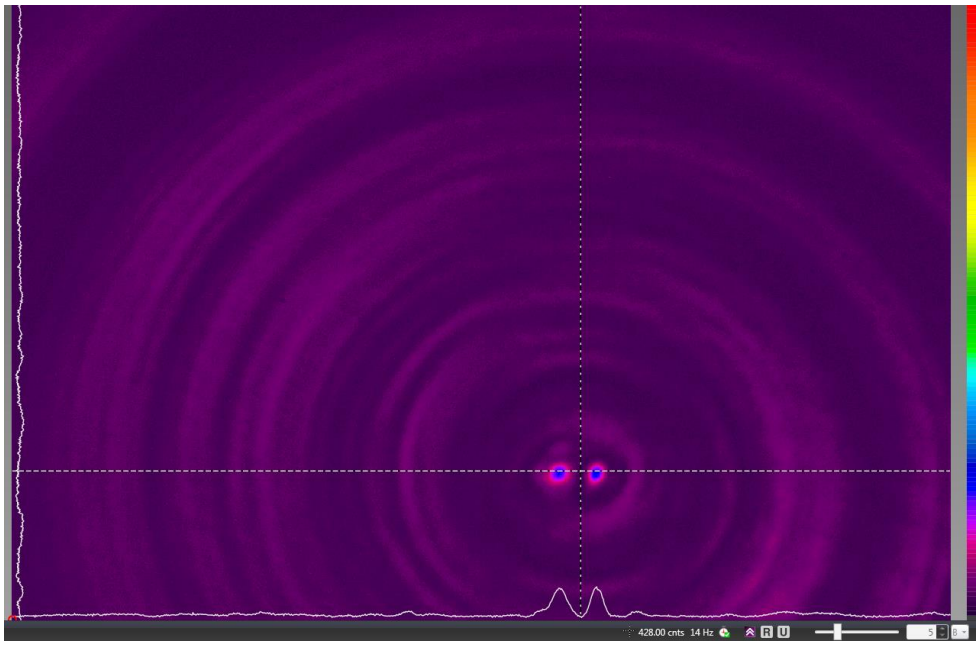

Fig. 4. The experimental diffraction pattern recorded at z_{tf}

To fabricate these microstructures in the aluminum layer of the holographic stamp, are required few technological conventional steps starting from a mask made in a photoresist layer transferred in a Ni shim. The final step consists in hot-embossing these microstructures in an aluminum layer. To introduce the designed phase shift in the optical path, it is required to control the

depth of the microrelief obtained in aluminum layer. For this reason, we performed the dynamic mechanical-thermal analysis (DMTA) for monitoring the behavior of the metallic layer with the change of the temperature under constant mechanical stress.

Dynamic mechanical-thermal analysis was performed on the aluminum layer covered with polyethylene terephthalate. (Fig. 5). These films were mounted in tension clamp with loading arranged so that the sample is always in tension. Dynamic mechanical analysis was carried out on a DMA –Q 800 (TA Instruments Inc., USA) , at a heating rate of 3°C min^{-1} from RT to 180 °C under air, 1Hz frequency and 4µm oscillation amplitude, initial sample length approx. 20 mm.

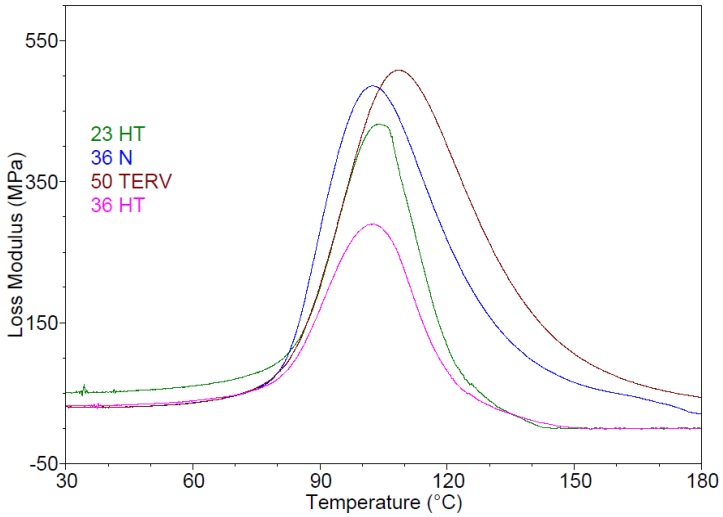

Fig. 5 DMA diagram of loss modulus vs. temperature

Below Tg – (glass transition temperature) from loss modulus peak maximum, the polymer (polyethylene terephthlate) is rigid and is able to resist the applied force, therefore its deformation is negligible. Above Tg, the polymer becomes soft and deformation was more. The temperature at which this occurs is called “softening temperature” and is highly dependent on the force applied to the sample.

Thermo-gravimetric analysis (TGA) was carried out on a TGA-Q5000IR (TA Instruments Inc., USA) between 30°C and 700°C at a heating rate of 10°C/min with nitrogen (99.999%) as purge gas at a flow rate of 50 ml/min. All the thermograms have similar shape, with two thermal events (Fig. 6). The first weight loss occurs between 160°C and 240°C and is probably due to the evaporation of some small molecular products (e.g. solvents). This weight loss is about 1.5% at 200°C for the first three samples, except for 50-TERV with only

0.5% but at a slightly higher temperature, 216°C, which can be better observed in the inset of derivative thermogravimetric (DTG) diagram. The major weight loss step occurs between 350°C and 500°C without major differences in both the maximum decomposition rate (in the range 431-436°C) and the residue with values between 13.5 and 15.3%. 50-TERV, apart from the low weight loss at 216°C, also differs through the decomposition onset parameters which is somewhat higher in both temperature (96°C) and weight (99.1%),

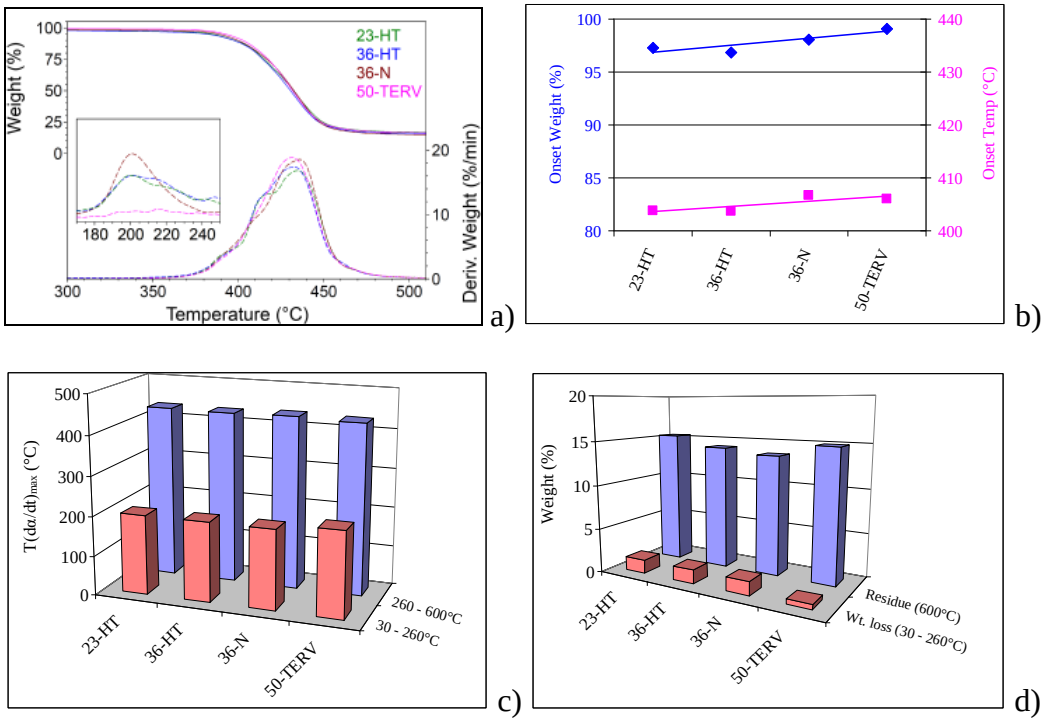

Fig. 6. Results of thermogravimetric analysis: a) TGA-DTG diagram; b) main decomposition onset parameters; c) temperature of maximum rates of decompositions; d) first decomposition weight loss and residues.

6. Discussions and conclusions

A simple method to obtain asymmetric Fresnel lenses AFLs and its effect on the focal spot are described. The asymmetry coefficient AC introduces displacement in the microstructures design of the order of hundreds of nanometers to few micrometers which modifies the apparent radius and transition points between zones. These changes in the geometry of the Fresnel lenses have consequences on the focal spots:

1) increasing of the FWHH values with AC, for spots located at z_f along propagation axis, and
2) twin focal spots located at z_{tf} along propagation axis; the distance between these twin focal spots increases with AC. This is a consequence of changing the transition points for odd and even zones, the area occupied by each zone is translated and the phase shift of 2π is spatially moved at new positions.

These simulation results are experimentally demonstrated using a spatial light modulator as test step before expensive fabrication in aluminum layer for holographic stamps.

Dynamic mechanical-thermal analysis was performed in controllable conditions, on samples used in the technological process to fabricate holographic stamps on aluminum layer. These analyzes are the first made on the samples of this kind and with few tens of micrometers thickness. This laboratory study is a precursor step before expensive fabrication and allows us to choose the optimal fabrication parameters for a given depth of the microrelief.

The AC introduces displacements of the order of submicrometric range in the AFLs geometry, impossible to detect by the human eye, but with effects in the reflected light. For this reason, these are proposed to be included for enhanced security features to be exploited for holographic stamps used as anti-counterfeit item on valuable objects. These are facilitated because AFLs are designed with only two levels and their microrelief is simple to imprint in aluminum layer using conventional technological processes.

In this proof of concept experiment we used a monochromatic source and we observed supplementary focal spots. In white light, colors separation as special visual effect become more spectacular, considering the fact that the diffractive lenses introduce inverse dispersion comparing with the refractive ones.

Acknowledgements

The research presented in this paper is supported by the Romanian Authority for Scientific Research Innovation, contr. UEFIS-CDI, PN-III -P2-2.1-PTE-2016-0072, No. 37PTE/2016.

R E F E R E N C E S

[1] *J. Albero, J. A. Davis, D. M. Cottrell, C. E. Granger, K. R. McCormick, I. Moreno*, "Generalized diffractive optical elements with asymmetric harmonic response and phase control," Appl. Opt., **vol. 52**, 2013, pp. 3637-3644

[2] *M Anguiano-Morales1, D. P. Salas-Peimbert1, G Trujillo-Schiaffino,• L. F. Corral-Martı´nez,,I Gardun˜o-Wilches*, "Generation of an asymmetric hollow-beam", Opt Quant Electron, **vol. 47**, 2015, 2983–2991

[3] *L. Ionel, D. Ursescu, L. Neagu, M. Zamfirescu*, "On-site holographic interference method for fast surface topology measurements and reconstruction", Phys. Scripta, **vol. 90**, no. 6, 2016, 065502
[4] *E. Scarlat, M. Mihailescu, A. Sobetkii*, "Spatial frequency and fractal complexity in single to triple beam", J. Opt. Adv. Mat., **vol. 12**, no. 1, pp. 105–109, 2010
[5] *C. Cîrtoaje, E. Petrescu, C. Moțoc* "Self-focusing in nematic liquid crystals subjected to magnetic fields", Optoelectron. Adv. Mat., **vol. 5**, no. 2, 2011, pp. 106-111
[6] *V. Stoian, C. Cîrtoaje, E. Petrescu, C. Motoc* "Nonlinearities induced by magnetic fields in nematic liquid crystals", Opt. Commun., **vol. 309**, 2013, pp. 286-290
[7] *M. V. N. S. Elikkottil, M. R Gupta, , B. Pesala*, "Asymmetric Diffraction Gratings for Color Shifting Structures," in *13th International Conference on Fiber Optics and Photonics*, OSA Technical Digest, 2016, paper Tu4A.11
[8] *A. Goncharsky, A. Goncharsky, S. Durlevich "*Diffractive optical element with asymmetric microrelief for creating visual security features", Opt. Expr., v**ol. 23**, no. 22, 2015, pp. 29184-29192
[9] *D. C. O'Shea, T. J. Suleski, A. D. Kathman, and D. W. Prather,* "Diffractive Optics: Design, Fabrication, and Test", SPIE Press, 2004
[10] *J.W. Goodman*, Introduction to Fourier Optics, Mc Graw-Hill Book Company, 1968
[11] *J. Garcia, D. Mas, and R.G. Dorsch*, "Fractional-Fourier-transform calculation through the fast-Fourier-transform algorithm", Appl. Opt., **vol. 35**, no. 3, 1996, pp. 7013–7018
[12] *M. Mihailescu, A. M. Preda, D. Cojoc, E.I. Scarlat, L. Preda*, Diffraction patterns from a phyllotaxis type arrangement, Optics and Lasers in Eng., **vol. 46**, no. 11, 2008, 802-809